JOURNAL OF AGRICULTURAL AND FOOD CHEMISTRY

Photolysis Pathway of Imazapic in Aqueous Solution: Ultrahigh Resolution Mass Spectrometry Analysis of Intermediates

M. HARIR,[†,||] A. GASPAR,[†] M. FROMMBERGER,[†] M. LUCIO,[†] M. EL AZZOUZI,[||] D. MARTENS,[‡] A. KETTRUP,[§] AND PH. SCHMITT-KOPPLIN*,[†]

GSF - National Research Center for Environment and Health, Institute of Ecological Chemistry, Ingoldstädter Landstraße 1, D-85764 Neuherberg, Germany,; LUFA, Obere Langgasse 40, 67346 Speyer, Germany,; Rumbecker Höhe 10, 59821 Arnsberg, Germany,; and University Mohamed V-Agdal, Faculty of Sciences, Av. Ibn Batouta, BP 1014 Rabat, Morocco

Direct degradation of imazapic, an herbicide of the imidazoline family, has been investigated in aqueous solution at different concentrations, pH values, and temperatures. The efficiency of the photodegradation process has been evaluated through degradation rate constants that could be fitted best with pseudo-first-order kinetics ($C_t = C_0\ e^{-kt}$). Ultrahigh resolution mass spectrometry (FTICR/MS) was used in electrospray ionization mode as a tool to study the photolysis process on a molecular level, whereas UV–vis and high-performance liquid chromatography/mass spectrometry analysis were used to follow, by time, the evolution of the intermediates. Taking advantage of the high resolving power of FTICR/MS to perform precise formula assignments taking account of the natural abundance of isotopes, we herein propose and demonstrate an approach using 2D-derived van Krevelen visualization (O/C, H/C, *m*/*z*) to confirm the formation of imazapic intermediates. Such an approach allows a qualitative analysis of intermediates and elucidates the plausible reaction pathways of the photolysis process. More than eight photoproducts were separated and identified as a phototransformation of the imidazole ring. A mechanistical pathway was proposed.

KEYWORDS: Photolysis; imazapic; kinetic; HPLC/MS; FTICR/MS; intermediates

1. INTRODUCTION

Over the past 30 years, owing to the extensive use of organic compounds in natural areas, the amount of pesticides in aqueous media has increased. Their elimination from natural waters is due to biotic and abiotic degradation. Photodegradation is one of the main pathways in the abiotic degradation of pesticides, and there is a need to clarify their degradation behavior. Because of the presence of some organic components at trace levels in natural environments, studying these species at the molecular level can be an analytical challenge, and laboratory setups are usually used.

Liquid chromatography coupled to mass spectroscopy (LC/MS) has been shown to be a powerful tool for the identification of degradation products in environmental samples (*1*). However, high-resolution techniques are usually needed to confirm molecular structure information. Fourier transform ioncyclotron resonance mass spectrometry (FTICR/MS) with electrospray ionization has been successfully applied to characterize natural organic matter and some of the most complex samples of biogeochemical origins (*2, 3*). Using this approach, a resolving power of more than 200000 with 200 ppb mass accuracy can be achieved, which allows for an exact determination of the elemental composition with only a few basic chemical constraints.

Imazapic (IUPAC name: (±)-2-[4,5-dihydro-4-methyl-4-(1-methylethyl)-5-oxo-1*H*-imidazol-2-yl]-5-methyl-3-pyridinecarboxylic acid) is a member of the imidazolinone family. Imidazolinones are used as selective herbicides (*4*): alfalfa, clover, peanuts, and certain trees and shrubs. According to the American Cyanamid Company that first commercialized imidazolinone herbicides, these chemicals are "some of the most potent herbicides on the market" (*5*). Upon application, they are rapidly taken up by plant roots and shoots and are rapidly transferred to other parts of the plant and accumulate in actively growing plant tissues (*6*). Imazapic is soluble in water and is not degraded hydrolytically in aqueous solution. There are few published articles focused on the abiotic degradation of the imidazolinone family and their intermediates.

Exposition of the aqueous solution of imazapic to simulated sunlight is a very useful tool for testing the susceptibility to photolysis with the aim of understanding the reaction pathways under natural conditions. In this work, a preliminary kinetic study of the photodegradation of imazapic was performed. The effects

* Author to whom correspondence should be addressed. Fax: (0049) 089 3187 3358. E-mail: schmitt-kopplin@gsf.de.
[†] GSF - National Research Center for Environment and Health.
[‡] LUFA.
[||] University Mohamed V-Agdal.
[§] Rumbecker Höhe.

10.1021/jf0720279 CCC: $37.00
Published on Web 10/26/2007

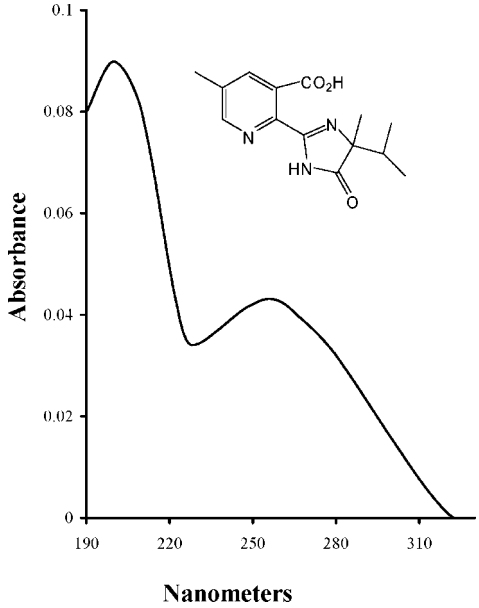

Figure 1. Chemical structure and UV/vis spectrum of imazapic.

Table 1. Values of Rate Constant of Degradation as a Function of Imazapic Concentrations during the Photolysis Process (30 °C, Natural pH)

concentration (mM)	K (10^{-3} min^{-1})	$t_{1/2}$ (min)	r^2
0.072	3.4	202.9	0.9967
0.14	3.7	186.4	0.9955
0.2	3.9	176.9	0.9984

of factors affecting the photodegradation such as herbicide concentration, pH, and temperature were investigated. UV–vis spectrometry, high-performance liquid chromatography/mass spectrometry (HPLC/MS), and FTICR mass spectrometry analysis were used to characterize the main intermediate products. In parallel, a possible photolytic degradation pathway of imazapic is proposed.

2. MATERIALS AND METHODS

2.1. Chemicals. Imazapic (**Figure 1**), purity > 99%, was purchased from Dr. Ehrenstofer (Augsburg, Germany). All solvents used for HPLC analysis were of chromatography grade, and all other chemicals were of analytical grade and were used without further purification. Water was purified using a Millipore-MilliQ system (Millipore, Billerica, MA).

2.2. Experimental Procedure. A stock solution of imazapic (0.36 mM) was prepared in pure water. For photodegradation studies, phosphate buffers (KH_2PO_4 and K_2HPO_4) were used. The solutions were buffed at pH 7.0, and then the pH_s was adjusted by the addition of NaOH or H_3PO_4. All irradiations of the solutions of imazapic were performed using a Heraeus (Hanau, Germany) Suntest CPS sunlight simulator (Xenon lamp; 290–800 nm; 765 Wm^{-2}). The lamp was positioned 20 cm apart from the cylindrical irradiation vessel. A Pyrex flask containing 50 mL of imazapic solutions was exposed to the simulated sunlight irradiation. Test controls were incubated in the dark to be sure that the transformation of imazapic was only due to light absorption. The solutions were homogenized by continuous stirring with a magnetic stirrer. For kinetic studies, samples from irradiated solutions were taken at regular time intervals and were analyzed directly by HPLC/diode array detection (DAD). The pH and temperature (30 °C) remained constant during photodegradation.

2.3. Degradation Rate Constant Determination and Calculation of Half-Life. The degradation of imazapic in the aqueous phase was modelled with a first-order kinetic. First-order rate constants "k" were determined from the slope of the linear plot of the natural logarithm of the imazapic concentration at various sampling intervals against the irradiation time.

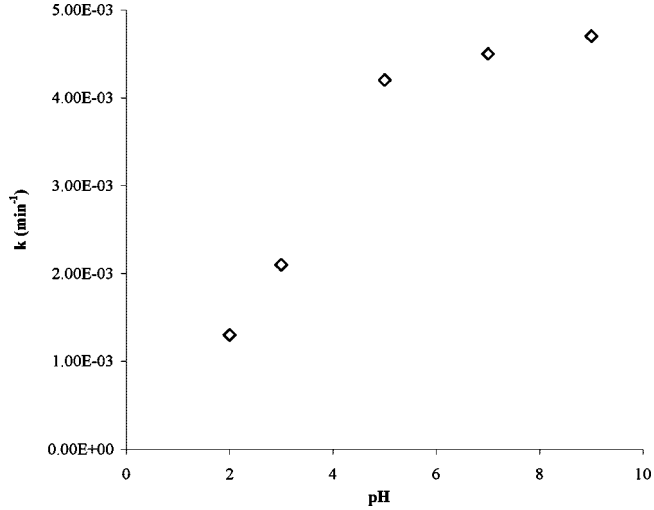

Figure 2. Effect of pH of the solution on the rate constant of degradation of imazapic (30 °C; 0.14 mM).

Table 2. Variation of the Rate Constant of Degradation of Imazapic as a Function of Temperature during the Photolysis Process (Natural pH, 0.14 mM)

temperature (°K)	K (10^{-3} min^{-1})	$t_{1/2}$ (min)	r^2
298	3.3	209.09	0.9886
303	3.7	186.40	0.9955
313	5.5	125.45	0.9894

The calculation of half-life (eq 1) was performed assuming the rate of the reaction to be first-order in herbicide concentration, by means of the kinetic equation

$$C_t = C_0 \, e^{-kt} \quad (1)$$

where C_t represents the concentration at time t, C_0 represents the initial concentration, and k is the photolytic rate constant. The fitting of the experimental data was satisfactory for all the samples. When the concentration is reduced to 50% of its initial value, the half-life ($t_{1/2}$) can be determined by

$$t_{1/2} = 0.693/k \quad (2)$$

3. ANALYSES

3.1. High-Performance Liquid Chromatography. HPLC/DAD was performed using a Perkin-Elmer Series 200 quaternary pump equipped with a 235C diode array detector, and a LiChrospher 100 RP-18 column (250 × 4 mm id, 5 μm) was used. The mobile phase was a mixture of water (pH = 3.0; H_3PO_4) and acetonitrile (80/20, v/v); the flow rate was 0.9 mL/min, and the injection volume was 20 μL. For UV–vis spectra, the DAD output from the HPLC experiments was used.

3.2. Liquid Chromatography/Mass Spectroscopy. The HPLC unit (Agilent Technologies, Palo Alto, CA) included a G1316A column oven, a G1329A autosampler with a thermostat (G1330A), a G1311A quaternary pump, and a G1322A degasser and was coupled with an API 2000 tandem mass spectrometer (Applied Biosystems, Toronto, Canada) equipped with an electrospray ionization (ESI) source. The chromatographic separation of the compounds was performed on a 75 × 2.0 mm (4 μm particle size) Synergy MAX-RP C12 column, provided with a 4 × 2.0 mm precolumn, both from Phenomenex (Aschaffenburg, Germany). The column oven temperature was 20 °C, and the flow rate was 300 μL/min. As eluents, methanol and ammonium carbonate (pH 5.0) were employed. The gradient

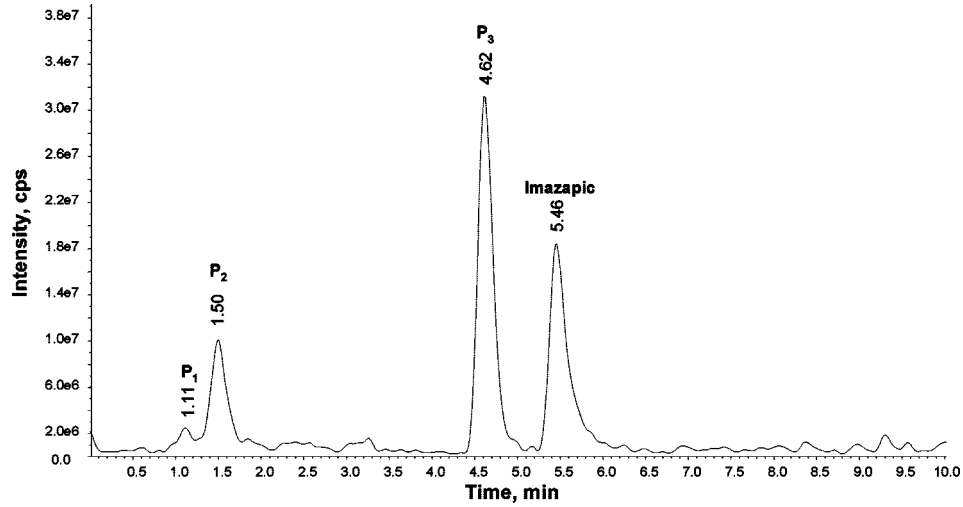

Figure 3. LC/MS chromatogram of degradation products of imazapic subjected to xenon lamp (see **Figure 6**). Pyrex reactor; column conditions: MeOH/amonium carbonate "ph5.0", 130 μL/min, 20 °C.

was increased from 10% to 100% methanol in 8 min, held for 1.40 min, then returned to the initial conditions and held until a total time of 14 min was reached, in order to equilibrate the column for the next run.

For system control and data acquisition, the Analyst software, version 1.4, from Applied Biosystems was used. The following source parameters were employed: TEM, 350 °C; CUR, 45 psi; IS, 1500 V; GS1, 50 psi; GS2, 60 psi. The focusing potential was optimized and fixed at 350 V. The compounds were fully scanned in the first quadrupole between 65 and 320 *m*/*z*, at a dwell time of 1 s. The entrance potential was fixed at 10 eV, whereas the declustering potential was varied between 10 and 30 eV. The focusing potential was set at 350 eV.

3.3. Fourier Transform Ion Cyclotron Resonance/Mass Spectrometry. High-resolution mass spectra for molecular formula assignment were acquired on a Bruker (Bremen, Germany) APEX Qe Fourier transform ion cyclotron resonance mass spectrometer (FTICR/MS) equipped with a 12 Tesla superconducting magnet and an APOLLO I ESI source. The samples were diluted in methanol to reach a concentration of 1 mg/L. For positive electrospray, water/methanol (50/50, v/v) was used. Samples were introduced into the microelectrospray source at a flow rate of 120 μL/h with a nebulizer gas pressure of 20 psi and a drying gas pressure of 15 psi (250 °C). Spectra were externally calibrated on clusters of arginine (10 mg/L in methanol) with a mass accuracy greater than 0.1 ppm. Spectra were acquired with a time domain of 1 megaword over a mass range of 100–600 *m*/*z*. For fragmentation experiments, ions were mass-selected between the ion source and the FTICR/MS analyzer with a quadrupole and fragmented by varying the collision voltage of the collision cell (CID). A total of 180 scans were accumulated for one spectrum.

3.4. Elemental Compositions. FTICR spectra were exported to peak lists. From those lists, possible elemental formulas were calculated for each peak in the batch mode by a software tool written in-house. The generated formulas were validated by setting sensible chemical constraints (N rule; O/C ratio $\leq$ 1; H/C ratio $\leq 2n + 2$; element counts, C $\leq$ 20, H $\leq$ 30, O $\leq$ 6, N $\leq$ 4), and the calculated formulas were considered valid only when the corresponding ^{13}C peak was detected in the spectrum.

4. RESULTS AND DISCUSSION

4.1. Preliminary Kinetic Study of Imazapic. *4.1.1. Effect of Concentration.* The photolysis of imazapic in aqueous solution at three different concentrations (0.072, 0.14, and 0.2 mM) was studied. Degradation of the herbicide under simulated sunlight irradiation showed the same tendency as a function of the remaining concentration and time of irradiation. The concentration of imazapic in the dark did not change during the experimental time. This is in agreement with the literature (*7*, *8*), where no hydrolysis reaction under similar conditions was observed. However, by increasing the herbicide concentration, slight variations in the rate constants of degradation were observed (**Table 1**). These changes were however too low to be considered as significant. These results suggest that there is no concentration effect in imazapic photodegradation as was previously observed for imazapyr (*9*).

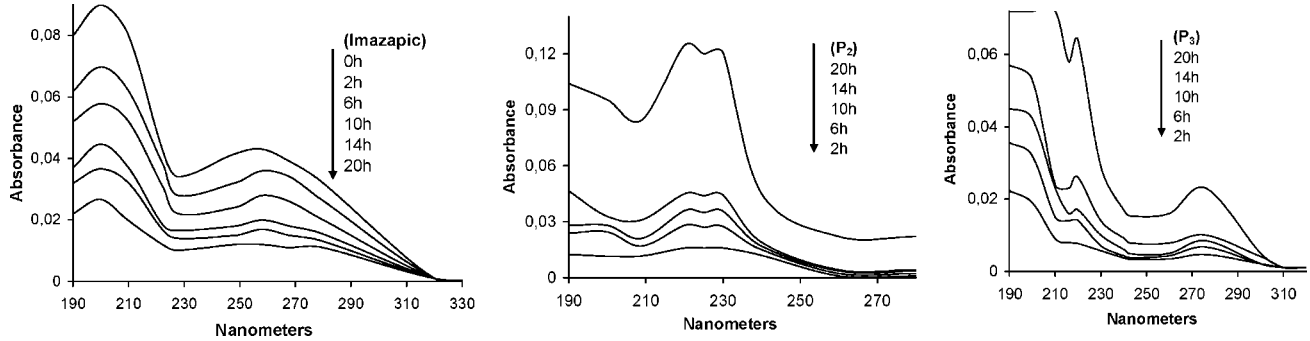

Figure 4. Absorbance spectral changes of imazapic and the byproducts (P_2) and (P_3) (see **Figure 3**) that occur during the photolysis process of an aqueous solution using HPLC/DAD.

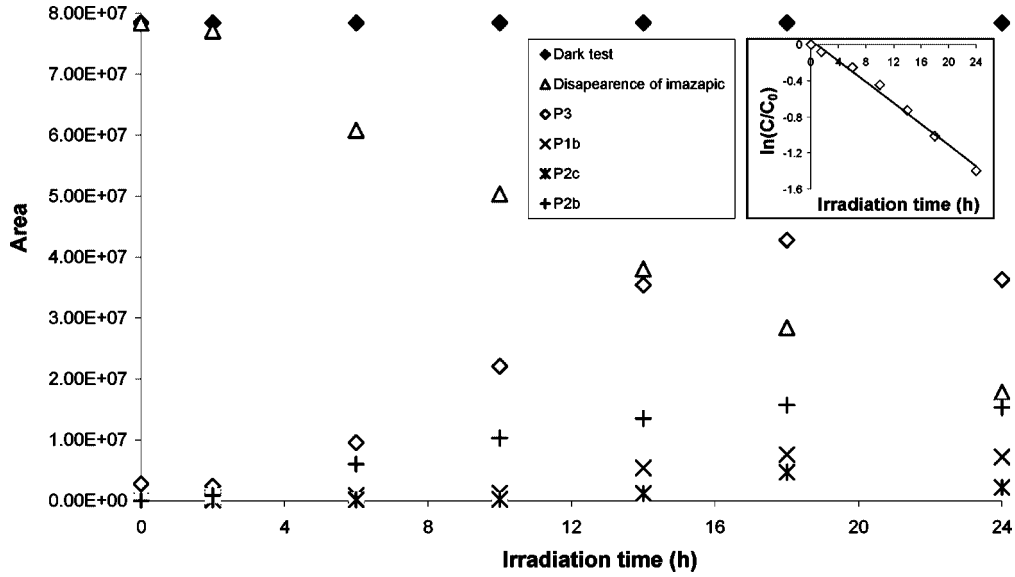

Figure 5. Evolution curve of imazapic degradation and its byproducts "xenon lamp, Pyrex reactor" (see **Table 3**). The insert shows the first-order linear transforms $\ln(C/C_0) = f(t)$ of imazapic degradation. Conditions: $C_0 = 0.14$ mM, $T = 30$ °C.

4.1.2. pH Effect. The effect of pH on the photolysis of imazapic using a solar UV simulator and a Pyrex reactor ($\lambda \geq 290$ nm) was studied in aqueous solution at pH values ranging from 2 to 9. The rate constant of degradation of imazapic increases as the pH of the reaction solution rises from 2 to 5; beyond 5, the rate appears to plateau, as shown in **Figure 2**. The disappearance of imazapic follows first-order kinetics, and the rate constants of degradation (0.8, 1.26, 4.1, 4.2, 4.2, 3.81, and 3.695×10^{-3} min^{-1}) were reached when the solution pH was varied between 2 and 9. As shown in **Figure 2**, the rates of degradation increase by increasing the pH and appear to plateau at pH $\geq$ 5. This could be explained probably by the fact that the molar absorption coefficients of the molecule are slightly higher at higher pH compared to the acidic pH (> pH 5). Similar behavior was reported for the degradation of imazaquin (*10*) and imazapyr (*8*).

4.1.3. Temperature Effect. Increased temperature is known to enhance the degradation of pesticides by accelerating both abiotic chemical reactions and microbial activity (*11–13*). The effect of temperature on imazapic photodegradation was studied at 25, 30, and 40 °C with a temperature accuracy of ±0.5 °C. As expected, the degradation of imazapic was significantly longer at 25 and 30 °C than at 40 °C (**Table 2**). The rates of degradation obtained showed results with slightly differing values at 25 (3.3×10^{-3} min^{-1}) and 30 °C (3.7×10^{-3} min^{-1})

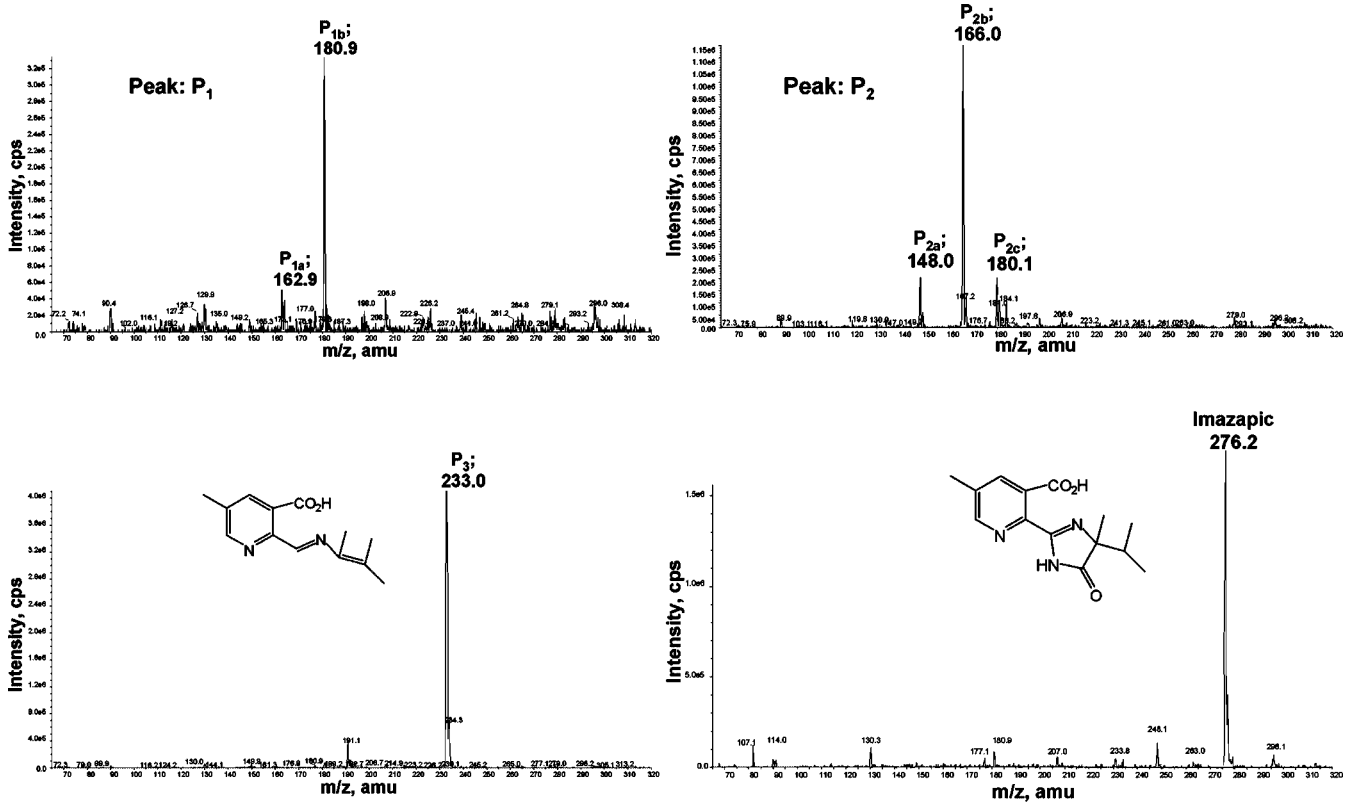

Figure 6. Extracted ion chromatogram of peaks P_1, P_2, P_3, and imazapic obtained from LC-MS analysis (**Figure 3**).

Table 3. FTICR/MS and LC/MS Analysis Data of Imazapic and Its Byproducts (in Positive Mode)[a]

	in FTICR-MS system					in LC/MS system	
intermediates	experimental mass	theoritical mass	error (±ppm)	^{13}C peaks	formula structure	extracted ion mass	t_r (min)
P_{1a}	163.05027	163.05020	0.404	164.05356[a]	$C_8H_7N_2O_2$	162.9	1.11
P_{1b}	181.06079	181.06077	0.115	182.06412[a]	$C_8H_9N_2O_3$	180.9	1.12
P_{2a}	148.03930	148.07930	0.400	*b*	$C_8H_6NO_2$	148.0	1.51
P_{2b}	166.04989	166.04987	0.120	167.05326	$C_8H_8NO_3$	166.0	1.50
P_{2c}	180.06554	180.06552	0.110	181.0689	$C_9H_{10}NO_3$	180.1	1.42
P_3	233.12844	233.12845	0.061	234.13181	$C_{13}H_{17}N_2O_2$	233.0	4.62
P_{3b}	191.08136	191.08150	0.755	192.08486[a]	$C_{10}H_{11}N_2O_2$	no[c]	
P_{4a}	164.03424	164.03422	0.121	165.04235[a]	$C_8H_6NO_3$	no	
P_{4b}	182.04482	182.04479	0.192	183.04817	$C_8H_8NO_4$	no	
P_5	248.13935	248.13935	0.013	249.14265	$C_{13}H_{18}N_3O_2$	no	
imazapic	276.13426	276.13427	0.030	277.13762	$C_{14}H_{18}N_3O_3$	276.2	5.46

[a] Small peaks. [b] Too small peak. [c] No: not extracted.

as compared to that at 40 °C (5.5×10^{-3} min^{-1}). However, temperature dependence implies that the degradation of pesticides, as in the case of imazapic, would increase in the hot seasons, volatilizing them from the water interface. For the same reasons, their degradation would decrease in cold seasons, where the risk of pesticide accumulation may increase. To simulate better laboratory conditions, a temperature of 30 °C was selected for further experiments.

4.2. Analysis of Photoproducts. *4.2.1. Photolysis.* HPLC/MS analyses were carried out in order to follow the main intermediates resulted from the photolytic process of imazapic. ESI in the positive mode was used to detect them. As described in **Figure 3**, the HPLC chromatogram shows the presence of three peaks corresponding to the intermediates P_1, P_2, and P_3 at retention times 1.11, 1.50, and 4.62 min, respectively. The imazapic peak appears at 5.62 min with a calculated half-life of 11.03 h^{-1}.

The gradual disappearance of imazapic and the appearance of the intermediates were monitored during the photolysis process by recording the UV spectra of samples in the 200–280, 320, and 330 nm ranges. Typical spectra are shown in **Figure 4**. The characteristic absorption almost begins to disappear after 20 h of irradiation time for imazapic (**Figure 4**), and begins to appear after 2 h of irradiation time for the intermediates (**Figure 4**; P_2 and P_3) under the experimental conditions.

When irradiated at $\lambda > 290$ nm, a 10 ppm imazapic aqueous solution was degraded quite slowly related to its kinetic of disappearance. After 2 h of irradiation, the remaining imazapic was ~98%. By increasing the time of irradiation, the amount decreased from ~77% in 6 h to ~48% after 14 h of irradiation. After one day, the amount had decreased to 22%, as shown in **Figure 5**.

The evolution and apparition of imazapic and its intermediates, respectively, as a function of the irradiation time is shown in **Figure 5**. We can clearly observe that the intermediates P_3 and P_{2b} are not stable under sunlight irradiation since they are in turn phototransformed. A maximum concentration was observed within 18 h of irradiation. For both intermediates P_{1b} and P_{2c}, a longer irradiation time is required to be sure of their evolution.

4.2.2. Extract Mass Ions Analysis. **Figure 6** shows extracted mass spectra of each peak present in LC/MS chromatogram (**Figure 4**). Five peaks at different retention times and with different *m*/*z* ratios were observed as compared with the blank sample at time zero. At retention time 4.62 min (**Figure 3**, P_3), a peak at $m/z = 233.0$ was extracted. By considering the retrosynthesis way, we suggest that this mass corresponds to the loss of one molecule of isocyanic acid (HNCO) due to the transposition of the α-proton of the imidazole ring (as shown before with imazamox (*14*)).

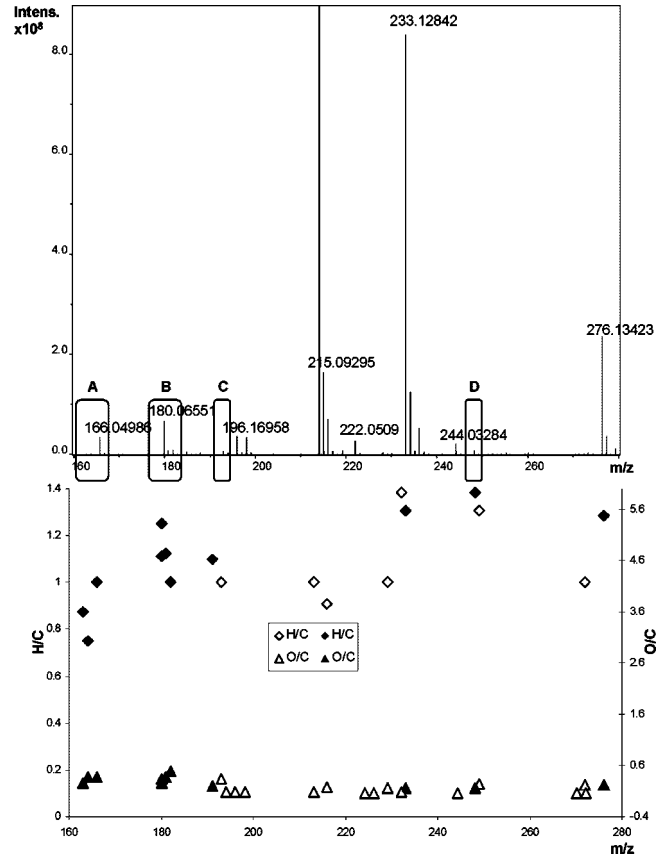

Figure 7. Visualization of 2D-derived Van Krevelen's diagram between theoretical (Δ, O/C; ◇, H/C) and experimental (▲, O/C; ♦, H/C) mass ratios of intermediates of imazapic in correlation with the FTICR mass spectrum of imazapic degradation (the signal-to-noise ratio of the basic peak is 8271:1).

The extracted ion chromatograms of $m/z = 148.0$, P_{2a}; $m/z = 166.0$, P_{2b}; and $m/z = 180.1$, P_{3c} (**Figure 6**) showed peaks with slightly different retention times, all contributing to the peak at around 1.5 min (**Figure 3**; P_2). For $m/z = 162.9$, P_{1a}, and 180.9, P_{1b} (**Figure 6**), the findings were similar (**Figure 3**; P_1). On the basis of the data obtained by LC/MS analysis (**Table 3**) and in the absence of availably standard compounds, we were unable to have a clear view of the intermediates produced. Consequently, a new investigation was used to clarify and to characterize the main intermediates of imazapic resulting from the photolysis process (see the FTICR/MS section).

4.3. FTICR-MS. *4.3.1. 2D-Derived Van Krevelen Diagrams Visualization.* Generally, Van Krevelen diagrams illustrate a plot of each elemental composition present in the FTICR mass

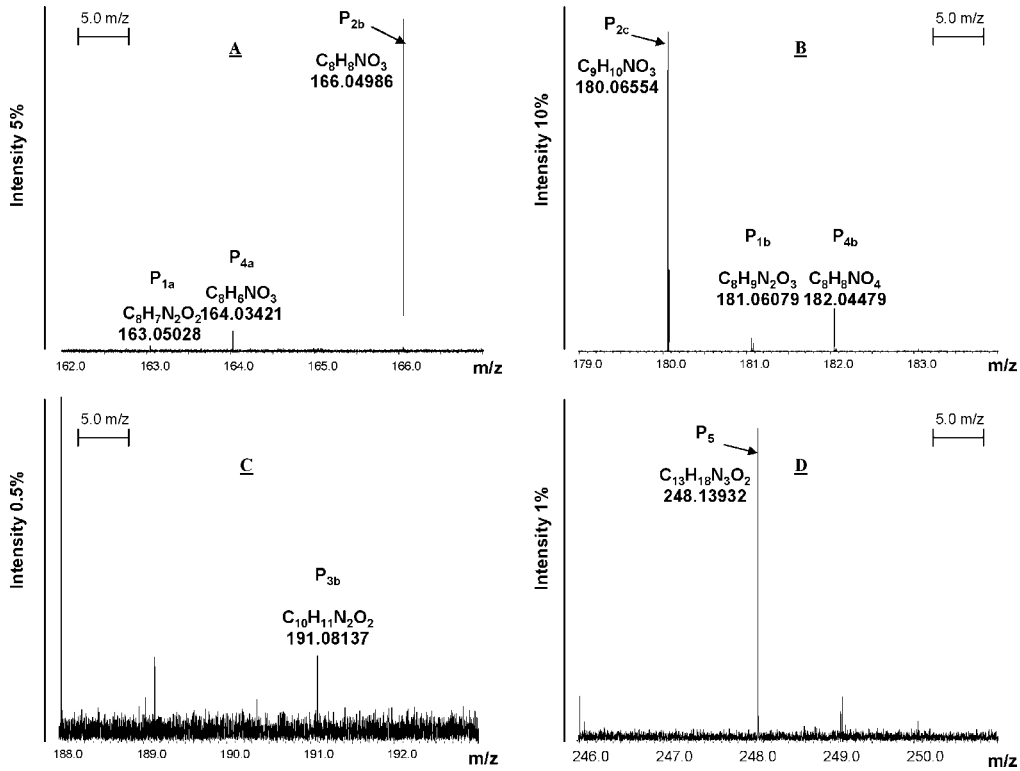

Figure 8. Mass scale of A, B, C, and D segments of intermediates at molecular masses of *m*/*z* 163.05027, 164.03424, 166.04989, 180.06554, 181.06079, 182.04482, and 248.13935 in the FTICR mass spectrum of **Figure 7** within the mass window *m*/*z* 5.0.

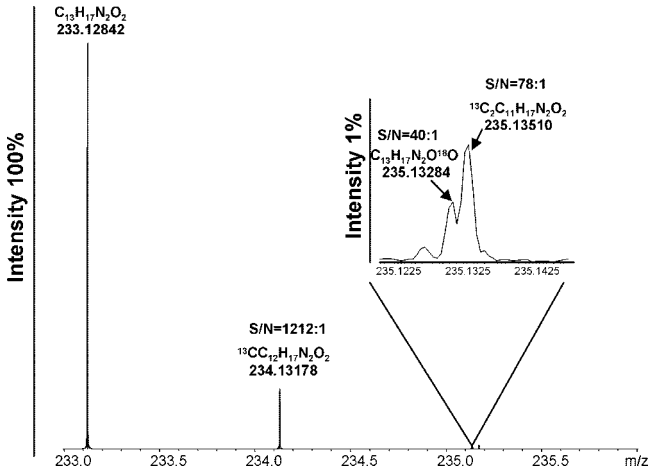

Figure 9. Further mass scale-expanded segment of the imazapic mass spectrum of **Figure 7**, allowing for the visual resolution and elemental composition assignment (on the basis of accurate mass measurement) of the natural abundance of isotopes of (*E*)-5-methyl-2-((3-methylbut-2-en-2-ylimino)methyl)nicotinic acid (its signal-to-noise ratio is 8271:1). The tabulated data for this byproduct show an average mass error of 0.062 ppm and a mass segment scale of *m*/*z* 3.0.

spectrum onto two or three axes according to its H/C, O/C, and/or N/C atomic ratios. The H/C ratio separates compounds according to the degree of saturation, whereas O/C or N/C ratios separate according to O and N classes (*15*). According to the results obtained in the case of imazamox (*14*), we herein propose and demonstrate a new approach using 2D-derived van Krevelen visualization to characterize the main intermediates of the photolysis process of imazapic. In the 2D-derived van Krevelen visualization, a plot is generated with the atomic ratio of hydrogen to carbon on the *y* axis, left; the ratio of oxygen to carbon on the *y* axis, right; and the nominal mass (*m*/*z*) of the intermediates on the *x* axis (**Figure 7**). At a given mass range, nine intermediates are observed with different elemental distributions and all of which were singly charged as proven by examination of the $^{12}C/^{13}C$ peak distance. By superimposing the FTICR mass spectrum (**Figure 7**) to a 2D-derived Van Krevelen plot, we can clearly observe the correlation existing between each separated group of intermediates related to the mass spectrum. On the basis of this applicable analysis, we are able, first, to attribute for each contribution of H/C and O/C ratio represented in a 2D-derived van Krevelen diagram an exact mass in the FTICR spectrum and, second, to separate all intermediate products from each other in silico without further classical separation (by, e.g., chromatography).

Additional interpretation requires mass scale expansion to resolve different elemental compositions at a given mass range (**Figure 8**). The mass accuracy available from FTICR/MS for ions' molecular mass ($[M + H]^+ = 163.05027$, 164.03424, 166.04989, 180.06554, 181.06079, 182.04482, and 248.13935) makes possible a unique assignment of elemental compositions for all seven of the resolved mass spectral peaks. Those elemental compositions in turn reveal the formula structure and the nature of the rupture.

4.3.2. Natural Abundance of 13 Carbon Isotopes of Imazapic. The relative natural abundance of stable isotopes associated with a given ionic species in a mass spectrum can be used as a diagnostic tool to distinguish between the various atomic combinations. Because of the natural abundance of carbon-13 (1.1%); nitrogen-15 (0.36%); and oxygen-18 (0.020%), several software packages are available for the analysis of mass spectrometry data. The dominance of carbon-13 isotopes was previously used to explain the even *m*/*z* peaks in high-resolution mass spectra of complex mixtures (*16*). Then, an investigation based on isotopes approach can offer a much greater understanding of the photolysis process of imazapic. As shown in **Figure 7**, all peaks observed in the FTICR mass spectrum of

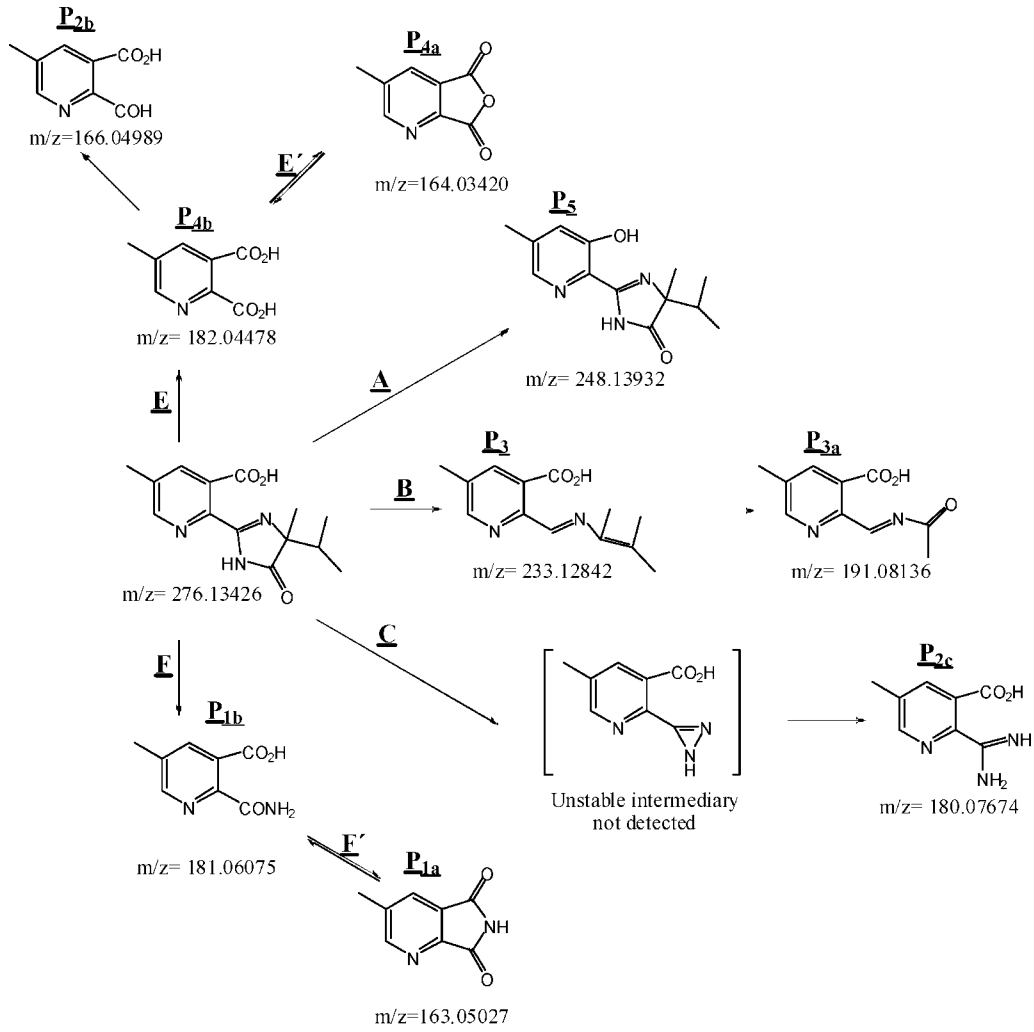

Figure 10. Degradation pathway proposed for the photolysis of imazapic in pure water.

imazapic are singly charged, and the principal equivalent isotopic masses of each intermediate are shown in **Table 3**.

As an example, the display of the abundant intermediate at $[M + H]^+ = 233.12844$ is shown in **Figure 9**. Every isotope has a unique, characteristic "mass defect"; so the mass of the ion, which shows the total mass defect, identifies its isotopic and elemental composition. This figure reveals the presence of $^{12}C_{13}$, $^{12}C_{12}{}^{13}C_1$, $^{12}C_{12}{}^{13}C_2$, and $^{12}C_{13}{}^{18}O^{16}O$ species corresponding to the natural abundance of isotopes of this intermediate ($C_{13}H_{17}N_2O_2$).

4.3.3. Proposed Degradation Pathways. Essentially, as described before with imazamox (*14*), the main intermediates of imazapic were identified and characterized by using ESI/FTICR mass spectrometry in the positive mode. It is known that high-resolution mass spectra permitted a determination of exact ions' mass values (*m*/*z*) and the elemental composition of each compound. On the basis of the fragmentation pathways analysis, a general schema of the photolysis process of the main intermediates is proposed in **Figure 10**. As a summary, **Table 3** shows the formula structure for the proposed degradation intermediates resulting from the photolysis of imazapic in pure water.

However, due to the high degree of photodecomposition of the imidazole ring under sunlight irradiation (*10*–*17*) and on the basis of a previous study (*14*), the main photoproducts obtained from the photolysis process of imazapic are most probably resultant from the pathways cited below.

Pathway A. The reduction of the acidic group by the loss of one carbon monoxide (C=O) fragment is the most probable route to obtain the 4-*tert*-butyl-2-(3-hydroxy-5-methylpyridin-2-yl)-4-methyl-1*H*-imidazol-5(4*H*)-one (P_5, $C_{13}H_{18}N_3O_2$; $[M + H]^+ = 248.13935$) intermediate as a decarbonylation process of imazapic.

Pathway B. The transposition of the α proton of the imidazole cycle leads to the formation of the (*E*)-5-methyl-2-((3-methylbut-2-en-2-ylimino)methyl) nicotinic acid (P_3, $C_{13}H_{17}N_2O_2$; $[M + H]^+ = 233.12844$) intermediate as shown in **Figure 10**. However, the reduction of the acidic group and the cleavage of ethylene bond (C=C) of the P_3 ($C_{13}H_{17}N_2O_2$) intermediate leads to the formation of (*E*)-2-((acetylimino)methyl)-5-(methoxymethyl)nicotinic acid (P_{3a}, $C_{10}H_{11}N_2O_2$; $[M + H]^+ = 191.08136$).

Pathway C. Initially, the cleavage of both amine and imine groups (=N–C and NH–C=O) may led to the formation of 2-(1H-diazirin-3-yl)-5-methylnicotinic acid (an unstable intermediary was not detected), as shown in **Figure 10**. Then, the opening of the 1*H*-diazirin-3-yl cycle is probably the only way to obtain the 2-carbamimidoyl-5-methylnicotinic acid (P_{2c}, $C_9H_{10}NO_3$; $[M + H]^+ = 180.06554$) intermediate.

Pathway F. The formation of 2-carbamoyl-5-methylnicotinic acid (P_{1b}, $C_8H_9N_2O_3$; $[M + H]^+ = 181.06079$) can be explained by the cleavage of both C=N and C–N bonds of the imidazole cycle. Whereas, the formation of the 3-methyl-5H-pyrrolo[3,4-

b]pyridine-5,7(6*H*)-dione (P_{1a}, $[M + H]^+ = 163.05027$; $C_8H_7N_2O_2$) intermediate can be explained by the loss of one water molecule, as excepted by the Nourish reaction (*18*).

Pathway E. The plausible structure of the 5-methyl-2,3pyridinecarboxylic acid (P_{4b}, $[M + H]^+ = 182.04482$; $C_8H_8NO_4$) intermediate is shown in **Figure 10**. In the absence of a hydrolysis reaction, the presence of this intermediate could be explained by the fact that light may modify (by a successive oxidation) the structure of the imidazole ring, and an enolic equilibrium in the ground state as well as in the first excited state could be envisaged (*10*). A similar degradation pathway has already been proposed for the photolysis of imazapyr (*17*) and imazamox (*14*). On the other hand, the formation of the 2-formyl-5-methylnicotinic acid (P_{2b}, $[M + H]^+ = 166.04989$; $C_8H_8NO_3$) intermediate could be interpreted by a reduction of the 5-methyl-2,3-pyridinecarboxylic acid compound.

Pathways E′ and F′. The loss of one water molecule from 5-methyl-2,3-pyridinecarboxylic acid (P_{4b}, $[M + H]^+ = 182.04482$; $C_8H_8NO_4$) and 2-carbamoyl-5-methylnicotinic acid (P_{1b}, $[M + H]^+ = 181.06079$; $C_8H_9N_2O_3$) intermediates leads to the formation of 3-methylfuro[3,4-b]pyridine-5,7-dione (P_{4a}, $[M + H]^+ = 164.03424$; $C_8H_6NO_3$) and 3-methyl-5*H*-pyrrolo[3,4-b]pyridine-5,7(6*H*)-dione (P_{1a}, $[M + H]^+ = 163.05027$; $C_8H_7N_2O_2$), respectively, as was the case for imazamox (*14*) and imazapyr (*17*). The presence of such intermediates could be explained by equilibrium between the cyclized and the opened forms in aqueous solution.

In summary, it was found that the photolysis efficiency of imazapic was more effective at higher pH and temperatures, but no significant concentration effect was observed. However, by combining the data from ultrahigh resolution mass spectrometry and liquid chromatography/mass spectrometry, nine intermediates were identified and characterized. The 2D-derived van Krevelen visualization is shown to be an effective and informative graphical method of analysis. This approach was usefully applied in the cases of imazamox (*14*), previously, and imazapic and could be taken as a general applied method to analyze similar degraded pollutants.

LITERATURE CITED

(1) Ferrer, I.; Thurman, E. M. Liquid Chromatography Mass Spectroscopy/Mass Spectroscopy, MS/MS and Time-of-Flight MS: Analysis of emerging Contaminants. *American Chemical Society Symposium Series 850*; Oxford University Press: Washington, DC, 2003.

(2) Brown, T. L.; Rice, J. A. Effect of Experimental Parameters on the ESI FT-ICR Mass Spectrum of Fulvic Acid. *J. Anal. Chem.* **2000**, *72*, 384–390.

(3) Fievre, A.; Solouki, T.; Marshall, A. G.; Cooper, W. T. High-resolution Fourier transform ion cyclotron resonance mass spectrometry of humic and fulvic acids by laser desorption/ionization and electrospray ionization. *Energy Fuels* **1997**, *11*, 554–560.

(4) Goatz, A.; Lavy, T.; Gbur, E. Degradation and field persistence of Imazethapyr. *Weed Sci.* **1990**, *38*, 421–489.

(5) Loux, M.; Liebl, R.; Slife, F. Avaibility and persistence of imazaquin, imazethapyr, and clomazone in soil. *Weed Sci.* **1989**, *37*, 259–267.

(6) Loux, M.; Reese, K. Effect of soil type and pH on persistence and carryover of imidazolinone herbicides. *Weed Technol.* **1993**, *7*, 259–267.

(7) Laifer, A. *The kinetics of environmental Aquatic Photochemistry*; American Chemical Society: Washington, DC, 1988; p 49.

(8) Mallipudi, N. M.; Stout, S. J.; da Cunda, A. R.; Lee, A. H. Photolysis of Imazapyr (AC 243997) Herbicide in Aqueous Media. *J. Agric. Food Chem.* **1998**, *39*, 412–417.

(9) El Azzouzi, M.; Mountacer, H.; Mansour, M. Kinetics of photochemical degradation of imazapyr in aqueous solution. *Fresenius Environ. Bull.* **1999**, *8*, 709–717.

(10) Barkani, H.; Catastini, C.; Emmelin, C.; Sarakha, M.; El Azzouzi, M.; Chovelon, J. M. Study of the phototransformation of imazaquin in aqueous solution: a kinetic approach. *J. Photochem. Photobiol., A.* **2004**, *170*, 27–35.

(11) Getzin, L. W. Factors influencing the persistence and effectiveness of chlorpyrifos in soil. *J. Econ. Entomol.* **1985**, *78*, 412–418.

(12) Racke, K. D. Environmental fate of chlorpyrifos. *Rev. Environ. Contam. Toxicol.* **1993**, *131*, 1–150.

(13) Bondarenko, S.; Gan, J. Degradation and sorption of selected organophosphate and carbamate insecticides in urban stream sediments. *Environ. Toxicol. Chem.* **2004**, *23*, 1809–1814.

(14) Harir, M.; Frommberger, M.; Gaspar, A.; Martens, D.; Kettrup, A.; El Azzouzi, M.; Schmitt-Kopplin, Ph. Characterization of Imazamox degradation by-products by using Liquid Chromatography Mass Spectrometry and High Resolution Fourier Transform Ion Cyclotron Resonance Mass Spectrometry. *Anal. Bioanal. Chem.* **2007**. [Online] DOI: 10.1007/s00216-007-1343-7.

(15) Wu, Z.; Rodgers, R. P.; Marshall, A. G. Two- and three-dimensional van krevelen diagrams: a graphical analysis complementary to the Kendrick mass plot for sorting elemental compositions of complex organic mixtures based on ultrahigh-resolution broadband fourier transform ion cyclotron resonance mass measurements. *Anal. Chem.* **2004**, *76*, 2511–6.

(16) Jan, S. P. Fourier Transform-Ion Cyclotron Resonance-Mass Spectrometer as a New Tool for Organic Chemists. *Synlett* **1999**, *2*, 249–266.

(17) Quivet, R.; Faure, J.; Georges, J. O. P.; Herbreteau, B. Kinetic study of imazapyr photolysis and characterization of the main photoproducts. *Toxicol. Environ. Chem.* **2004**, *86*, 197–206.

(18) Norrish, R. G. W.; Bamford, C. H. Photodecomposition of aldehydes and ketones. *Nature* **1937**, *140*, 195.

Received for review July 6, 2007. Revised manuscript received August 30, 2007. Accepted August 30, 2007. The authors thank the German Academic Exchange Service (DAAD) for a grant to M.H. and the German–Israeli Foundation for Scientific Research and Development (GIF) for financial support of M.H. and M.F.

JF0720279